Int J Cardiovasc Imaging (2015) 31:585–593
DOI 10.1007/s10554-014-0571-0

ORIGINAL PAPER

# Endothelial shear stress estimation in the human carotid artery based on Womersley versus Poiseuille flow

**Janina C. V. Schwarz · Raphaël Duivenvoorden · Aart J. Nederveen · Erik S. G. Stroes · Ed VanBavel**

Received: 26 August 2014 / Accepted: 10 November 2014 / Published online: 18 November 2014


**Abstract** Endothelial shear stress (ESS) dynamics are a major determinant of atherosclerosis development. The frequently used Poiseuille method to estimate ESS dynamics has important limitations. Therefore, we investigated whether Womersley flow may provide a better alternative for estimation of ESS while requiring equally simple hemodynamic parameters. Common carotid blood flow, centerline velocity, lumen diameter and mean wall thickness (MWT) were measured with 3T-MRI in 45 subjects at three different occasions. Mean ESS and two measures of pulsatility [shear pulsatility index (SPI) and oscillatory shear index (OSI)] were estimated based on Poiseuille and Womersley flow and compared to the more complex velocity gradient modelling method. The association between ESS and MWT was tested with multiple linear regression analysis; interscan reproducibility was assessed using intraclass correlation coefficients (ICC). Mean ESS and pulsatility indices based on Womersley flow ($ESS_{wq}$ $\beta = -0.18$, $P = 0.04$; $SPI_{wq}$ $\beta = 0.24$, $P = 0.02$; $OSI_{wq}$ $\beta = 0.18$, $P = 0.045$), showed equally good correlations with carotid MWT as the velocity gradient method ($ESS_{vg}$ $\beta = -0.23$, $P = 0.01$; $SPI_{vg}$ $\beta = 0.21$, $P = 0.02$; $OSI_{vg}$ $\beta = 0.07$, $P = 0.47$). This in contrast to the Poiseuille flow method that only showed a good correlation for mean ESS ($ESS_{pq}$ $\beta = -0.18$, $P = 0.04$; $SPI_{pq}$ $\beta = 0.14$, $P = 0.14$; $OSI_{pq}$ $\beta = 0.04$, $P = 0.69$). Womersley and Poiseuille methods had high intraclass correlation coefficients indicating good interscan reproducibility (both ICC = 0.84, 95 % confidence interval 0.75–0.90). Estimation of ESS dynamics based on Womersley flow modelling is superior to Poiseuille flow modelling and has good interscan reproducibility.

**Keywords** Endothelial shear stress · Cardiovascular magnetic resonance · Common carotid artery · Intima media thickness

**Abbreviations**

| | |
|---|---|
| 3T-MRI | 3.0 Tesla magnetic resonance imaging |
| ESR | Endothelial shear rate |
| ESS | Endothelial shear stress |
| ICC | Intraclass correlation coefficient |
| LA | Lumen area |
| MWT | Mean wall thickness |
| OSI | Oscillatory shear index |
| Q | Blood flow rate |
| SPI | Shear pulsatility index |
| v | Centerline velocity |

Janina C. V. Schwarz and Raphaël Duivenvoorden have contributed equally.

**Electronic supplementary material** The online version of this article (doi:10.1007/s10554-014-0571-0) contains supplementary material, which is available to authorized users.

J. C. V. Schwarz · E. VanBavel (✉)
Department of Biomedical Engineering and Physics, Academic Medical Center, University of Amsterdam, Amsterdam, The Netherlands
e-mail: e.vanbavel@amc.uva.nl

R. Duivenvoorden · E. S. G. Stroes
Department of Vascular Medicine, Academic Medical Center, University of Amsterdam, Amsterdam, The Netherlands

A. J. Nederveen
Department of Radiology, Academic Medical Center, University of Amsterdam, Amsterdam, The Netherlands

## Introduction

Endothelial shear stress (ESS) is the hemodynamic force that flowing blood exerts on the vessel wall [1]. This force is continuously sensed by mechanoreceptors that are attached to the cytoskeleton of endothelial cells [2]. Processes involved in endothelial cell turnover, inflammation, coagulation, extracellular matrix degradation, and production of vasoactive substances such as nitric oxide are all tightly regulated by ESS [1–4]. In vitro and animal studies showed that protracted decrease in ESS and high variation of ESS during the cardiac cycle cause endothelial receptor and gene expression to switch to an atherogenic phenotype [1–4]. Vascular imaging studies corroborate these findings, showing a causal relationship between ESS and atherosclerosis development [5–8].

Assessing ESS in vivo is technically challenging, which is the reason why human studies on ESS remain scarce, and are typical performed in small sample sizes. Various methods are used, including computational fluid dynamics, velocity gradient modelling, and methods assuming Poiseuille flow [9]. Computational fluid dynamics can solve the Navier–Stokes equations of fluid flow [9], while velocity gradient modelling is based on the spatial gradient of the velocities close to the artery wall using second-order curve fitting of the velocity profile [5, 9, 10]. Although accurate methods, their downsides pertain to the fact that high resolution information is needed on the local velocity vector throughout the cycle, respectively as boundary condition for the Navier–Stokes equations and as base for the accurate fitting of the velocity gradient perpendicular to the wall. Obtaining such data is labor intensive and dedicated software is needed for the complex data analysis, which is not freely available. In contrast, Poiseuille based methods are simpler as they merely require measurement of artery diameter and flow rate or centerline velocity followed by a simple calculation [9]. Estimation of ESS dynamics are then based on the instantaneous hemodynamics during the cycle. However, Poiseuille flow requires among others steady flow in straight rigid tubes. These conditions are violated in vivo in human arteries, resulting in deviation from the assumed parabolic velocity profile [9, 11]. Despite the inherent inadequacy of Poiseuille based methods, the majority of current literature relies on this approach due to its simplicity and availability [6–8, 12, 13].

Therefore, we investigated whether an equally simple method based on similar parameters (diameter and flow rate or centerline velocity) provides a better alternative to the Poiseuille based method. This method is based on Womersley flow [14], which in contrast to Poiseuille covers pulsatile flow components. We compared the Womersley method to the Poiseuille based method as well as to velocity gradient modelling from high resolution phase contrast (PC)-MRI. We correlated ESS of each method with carotid artery wall thickness, assuming that higher correlations are obtained with more accurate ESS estimations [15]. We also compared reproducibility of each of the methods. All measurements were performed in the common carotid arteries by 3T-MRI.

## Methods

### Subject population

Forty-five subjects (age range 19–79 years) were enrolled prospectively. The population consisted of 30 volunteers and 15 patients with cardiovascular disease who were selected from the outpatient clinic of the Department of Vascular Medicine of the Academic Medical Center, Amsterdam, The Netherlands. In all subjects repeat 3T-MRI scans were acquired on three separate occasions, 1–3 weeks apart. All image analyses were done off-line. Prior to the studies, approval was obtained from the institutional review board of the Academic Medical Center, Amsterdam, The Netherlands. All subjects gave written informed consent.

### Image acquisition

Magnetic resonance imaging scans were obtained bilaterally on a 3T-MRI scanner (Intera, Philips Medical Systems, Best, The Netherlands) using a single-element microcoil (Philips, Hamburg, Germany) with a diameter of 5 cm. Axial magnetic resonance angiography images were acquired using a time of flight sequence to localize the left and right common carotid artery and position the scan planes perpendicular to the vessel.

For hemodynamic assessments, axial gradient echo phase-contrast images were acquired with a temporal resolution of 17 ms, and temporal interpolation was performed by the scanner software to 60 phases per heartbeat (retrospective electrocardiography gating). The scan plane was positioned 27 mm proximal to the carotid flow divider. Sequence parameters were: slice thickness 3 mm, non-interpolated pixel size $0.65 \times 0.65$ mm, field of view $60 \times 60$ mm, velocity encoding 150 cm $s^{-1}$ (unidirectional), repetition time 8.1 ms, echo time 5 ms, flip angle 10°, number of signal averages 2, total scan time 3–4 min. Both magnitude images and velocity encoded phase images were reconstructed.

To assess carotid wall thickness, axial T1-weighted Turbo Spin Echo image stacks were acquired at end-

diastole using double inversion recovery black blood preparation applying active fat suppression (spectral attenuated inversion recovery technique) as described previously [5]. Sequence parameters were: slice thickness 3 mm, imaging matrix size 240, field of view of 60 × 60 mm, noninterpolated pixel size 0.25 × 0.25 mm, echo time 9 ms, repetition time according to the subjects' heart rate (approximately 900 ms), echo train length 7, echo train duration 63 ms. All imaging was performed with cardiac gating.

### Image analysis

For assessment of hemodynamic parameters in the carotid arteries, off-line semi-automated qualitative and quantitative image analysis was performed using software written in Matlab developed at the Academic Medical Center, Amsterdam, The Netherlands. The lumen area (LA, $mm^2$) of all 60 phases per cardiac cycle was assessed by automated tracing of the lumen-wall boundaries on the gradient echo images [16]. The velocity at each pixel in the artery lumen was measured, which enabled the calculation of the volumetric flow rate (Q, $cm^3\ s^{-1}$) and centerline velocity (v, $cm\ s^{-1}$) of each phase in the cardiac cycle. The measured lumen area, flow rate, and centerline velocity were used to calculate the Poiseuille and Womersley based endothelial shear rate (ESR, $s^{-1}$). The calculations are shown in the Supplementary Methods. While Poiseuille and Womersley should predict identical mean ESS, a very minor difference exists in the data due to taking respectively an actual and a time-averaged diameter for the calculations. For the assessment of ESR based on the velocity gradient modelling method, we used dedicated software written in Matlab developed at the Academic Medical Center, Amsterdam, The Netherlands. We have described the method in detail previously [5]. Firstly, the lumen area (LA, $mm^2$) of all 60 phases per cardiac cycle was assessed as described above. Secondly, for each pixel the shortest distance to the artery wall was calculated. The lumen-wall boundaries were projected on the velocity encoded images. The ESR was assessed by determining the spatial gradient of the velocities close to the artery wall using second order curve fitting of the velocity profile. The pixels located from 0.31 to 1.56 mm from the wall were included for the analysis. The fit was forced to include the position of the artery wall with a velocity of zero to conform to the zero-slip condition.

For all methods (Poiseuille, Womersley and velocity gradient modelling), ESR was multiplied with the blood viscosity to calculate the ESS throughout the cardiac cycle. Blood viscosity was assumed to be 3.2 cP [17]. Poiseuille and Womersley methods were either based on flow rate ($ESS_{pq}$, $ESS_{wq}$) or centerline velocity ($ESS_{pv}$, $ESS_{wv}$).

From these dynamics, we calculated the mean ESS of all phases in the cardiac cycle as well as the shear pulsatility index (SPI) and the oscillatory shear index (OSI). SPI was defined as difference between the maximum and minimum ESS in the cardiac cycle divided by their sum. The oscillatory shear index represents the proportion of shear stress deviating from its predominant direction during the cardiac cycle [18].

For the carotid wall thickness quantification, semiautomated image analysis was performed using VesselMass software (Leiden University Medical Center, Leiden, The Netherlands). VesselMass performed automated tracing of the lumen-wall boundaries and the outer wall boundaries. The software algorithm for boundary detection and analysis methods are described elsewhere [19, 20].

### Statistical analysis

Continuous variables are expressed as means ± standard deviations (SD). We used multiple linear regression analysis to assess the association between the ESS values and MWT with MWT as the response variable and ESS as the explanatory variable. We determined by stepwise analysis with backward elimination that age and systolic blood pressure were the only significant confounders among all measured cardiovascular risk factors (patient characteristics and biochemistry as listed in Table 1). We therefore adjusted for these confounders. The agreement between successive ESS estimations was assessed using intraclass correlation coefficients (ICC) and the 95 % confidence intervals of the ICCs. For all statistical analyses Statistical Package for the Social Sciences version 20.0 for Windows was used.

## Results

Three MRI scans were performed in all 45 subjects. The population consisted of 20 females and 25 males. Their characteristics are shown in Table 1. Figure 1 shows two examples of wall thickness (Fig. 1a, d), measured peak systolic flow velocity (color scales in Fig. 1b, c, e, f), and estimations of peak systolic flow velocity based on Poiseuille (Fig. 1b, e) and Womersley (Fig. 1c, f) with flow rate as input. As can be seen, both vessels were approximately circular and measured flow velocity was relatively axisymmetric in both examples. The Womersley-based prediction far more closely matched the measured profile as compared to the Poiseuille-based estimate. The Womersley but not the Poiseuille model predicted flow reversal at the wall (OSI > 0), while in these cases the thicker wall was associated with a larger $OSI_{wq}$. Average data for common carotid lumen area, mean wall thickness

**Table 1** Volunteer characteristics, hemodynamics and ESS estimates

| | (N = 45) |
|---|---|
| Patient characteristics | |
| Age (years) | 48.9 (17.6) |
| Male gender (n, %) | 26 (58) |
| Body Mass Index (kg $m^{-2}$) | 24 (22–26) |
| Smokers (n, %) | 5 (11) |
| Cardiovascular disease (n, %) | 15 (33) |
| Biochemistry | |
| Total Cholesterol (mmol $l^{-1}$) | 4.7 (3.9–5.5) |
| Low density lipoprotein cholesterol (mmol $l^{-1}$) | 2.5 (1.9–3.5) |
| High density lipoprotein cholesterol (mmol $l^{-1}$) | 1.6 (0.4) |
| Triglycerides (mmol $l^{-1}$) | 0.8 (0.6–1.1) |
| Fasting glucose (mmol $l^{-1}$) | 5.2 (0.7) |
| Carotid wall and lumen | |
| Carotid lumen area ($mm^2$) | 34.0 (8.4) |
| Carotid wall thickness (mm) | 0.72 (0.23) |
| Hemodynamic parameters | |
| Heart rate ($min^{-1}$) | 64 (10) |
| Systolic blood pressure (mmHg) | 127 (15) |
| Diastolic blood pressure (mmHg) | 73 (7) |
| Mean carotid flow ($cm^3$ $s^{-1}$) | 6.27 (1.14) |
| Peak carotid centerline velocity (cm $s^{-1}$) | 71.14 (14.42) |
| Velocity gradient modelling | |
| Mean $ESS_{vg}$ (N $m^{-2}$) | 0.87 (0.25) |
| $SPI_{vg}$ (−) | 0.82 (0.12) |
| $OSI_{vg}$ (−) | 0.001 (0.004) |
| Womersley, center line velocity | |
| Mean $ESS_{wv}$ (N $m^{-2}$) | 0.63 (0.15) |
| $SPI_{wv}$ (−) | 1.67 (0.41) |
| $OSI_{wv}$ (−) | 0.083 (0.055) |
| Womersley, flow | |
| Mean $ESS_{wq}$ (N $m^{-2}$) | 0.76 (0.19) |
| $SPI_{wq}$ (−) | 1.30 (0.21) |
| $OSI_{wq}$ (−) | 0.026 (0.021) |
| Poiseuille, center line velocity | |
| Mean $ESS_{pv}$ (N $m^{-2}$) | 0.63 (0.15) |
| $SPI_{pv}$ (−) | 0.60 (0.08) |
| $OSI_{pv}$ (−) | 0.000 (0.000) |
| Poiseuille, flow | |
| Mean $ESS_{pq}$ (N $m^{-2}$) | 0.73 (0.18) |
| $SPI_{pq}$ (−) | 0.67 (0.08) |
| $OSI_{pq}$ (−) | 0.000 (0.001) |

Mean (± SD) values or median (interquartile range) values for non-normal distributions for volunteer characteristics, biochemistry, hemodynamic parameters, and carotid wall and lumen parameters measured by 3T-MRI (reported previously). ESS is endothelial shear stress, SPI is shear pulsatility index and OSI is oscillatory shear index

(MWT, mm), hemodynamic parameters, and ESS parameters are shown in Table 1. Mean ESS is by definition equal when based on Poiseuille or Womersley flow, and these estimates were comparable to the estimate from velocity gradient modelling. SPI for the Womersley based methods was around twice as high as that for the other methods. The amount of negative shear stress as assessed with OSI was low for all methods with Womersley based methods exhibiting the highest values (Table 1). In particular, the $OSI_{pv}$ was constantly zero such that its reproducibility and correlation with MWT could not be assessed. Figure 2 shows the different ESS estimates throughout the cardiac cycle averaged for all subjects.

Partial regression coefficients between ESS, SPI and OSI values and MWT, adjusted for the potential confounders age and systolic blood pressure, are shown in Table 2. The mean ESS and SPI of the velocity gradient modelling and Womersley flow rate based modelling methods correlated equally well with MWT, while only the mean ESS of the Poiseuille flow rate based method correlated with MWT. The OSI of both Womersley methods (either based on flow rate or centerline velocity) correlated with MWT. The Poiseuille centerline velocity based method did not show any good correlations with MWT. The interscan variabilities of the different methods are shown in Table 3. Womersley and Poiseuille based methods tended to have higher intraclass correlation coefficients than the velocity gradient modelling methods, indicating better interscan reproducibility.

## Discussion

In the present study we show that for estimation of dynamic ESS from flow rate or centerline velocity in the common carotid artery, methods based on Womersley outperform Poiseuille based methods. Furthermore we show that flow rate-based methods perform better than centerline velocity-based methods. We base these conclusions on the correlation of predicted ESS with the mean wall thickness of the vessel. A third method, based on the velocity gradient near the wall, also predicted ESS that correlates with MWT, but this method requires detailed information on the flow pattern, which is not commonly available. All methods had good interscan reproducibility. Our findings implicate that the easily applicable Womersley based method enables better ESS, SPI and OSI estimation in future clinical studies and can replace the currently frequently used Poiseuille based methods.

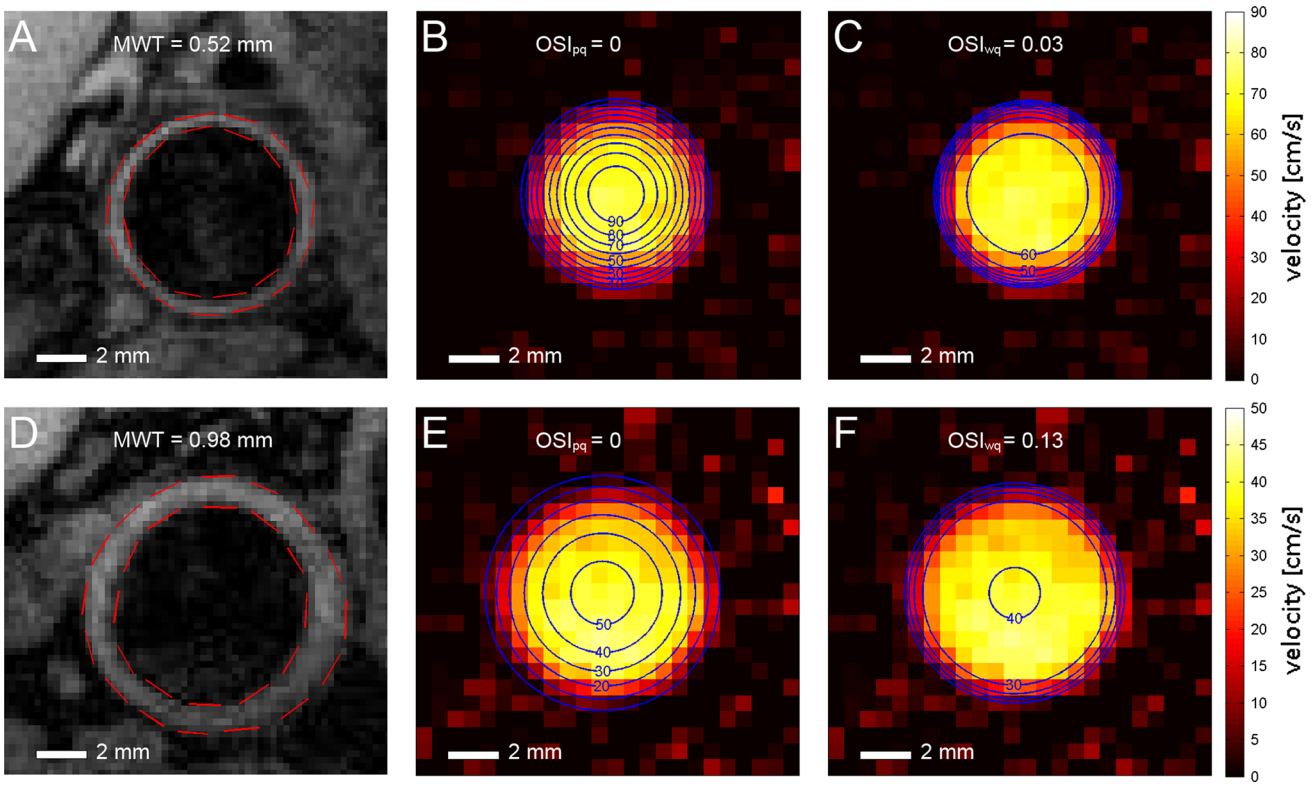


**Fig. 1** Two examples of measured mean wall thickness (MWT, **a**, **d**) and peak systolic flow velocity profiles with their Poiseuille- and Womersley-based estimates. The phase contrast MRI-based velocity profiles are shown as color-coded image (**b**, **c**, **e**, **f**). Estimated profiles are indicated as contour plots. **b**, **e** Poiseuille-based with flow rate as input, **c**, **f** Womersley-based with flow rate as input. OSI: estimated oscillatory shear index

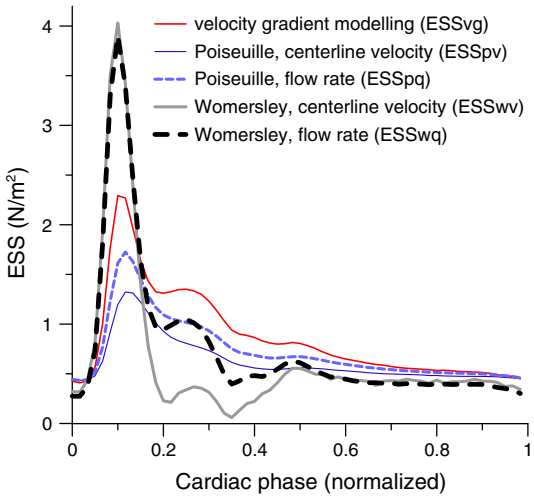


**Fig. 2** Common Carotid Endothelial Shear Stress (ESS, N m$^{-2}$) during the cardiac cycle averaged for all subjects for all estimation methods (*red* velocity gradient modelling method, *blue* Poiseuille flow modelling based on centerline velocity, *interrupted blue* Poiseuille flow modelling based on flow rate, *grey* Womersley flow modelling based on centerline velocity, *interrupted black* Womersley flow modelling based on flow rate). Per cardiac cycle, 60 image frames were made where the first frame coincided with the R wave of electrocardiogram. ESS was quantified for all 60 frames per heartbeat

Womersley theory is far from new [14, 21]. Yet, it is not commonly applied for estimation of ESS parameters [22] with few in vivo applications [23–26], and studies on the correlation with MWT in the common carotid arteries were lacking. The fundamental difference between Poiseuille and Womersley flow is that the latter takes the inertia of blood into account. This effect of inertia depends on the flow dynamics and the geometry and is known to be substantial for common carotid arteries [27]. For the mean ESS, inertia is not relevant and Poiseuille and Womersley provide identical estimates.

A low time-averaged ESS is considered to be atherogenic [3, 6–8, 28–30]. We indeed observed that low mean ESS, when using the flow rate as input, or based on the velocity gradient method, correlated with a thicker wall. We did find differences in estimates for mean ESS between the methods. In particular, using centerline velocity as input predicted lower values, which also were no longer correlated with MWT. This may be caused by more inherent noise in centerline velocity as compared to the flow rate, as well as by systematic deviations of the time-averaged velocity field from an axisymmetric parabolic profile, towards a flatter profile. For flow rate as input, the

**Table 2** Relation between endothelial shear stress and carotid wall thickness

| | Beta coefficient | 95 % CI | *P* |
|---|---|---|---|
| Velocity gradient modelling | | | |
| Mean $ESS_{vg}$ | −0.23 | −0.35 to −0.05 | 0.01 |
| $SPI_{vg}$ | 0.21 | 0.06 to 0.66 | 0.02 |
| $OSI_{vg}$ | 0.07 | −6.64 to 14.23 | 0.47 |
| Womersley, center line velocity | | | |
| Mean $ESS_{wv}$ | −0.13 | −0.45 to 0.09 | 0.19 |
| $SPI_{wv}$ | 0.23 | 0.02 to 0.23 | 0.02 |
| $OSI_{wv}$ | 0.19 | 0.03 to 1.41 | 0.04 |
| Womersley, flow | | | |
| Mean $ESS_{wq}$ | −0.18 | −0.42 to −0.01 | 0.04 |
| $SPI_{wq}$ | 0.24 | 0.04 to 0.47 | 0.02 |
| $OSI_{wq}$ | 0.18 | 0.04 to 3.61 | 0.045 |
| Poiseuille, center line velocity | | | |
| Mean $ESS_{pv}$ | −0.13 | −0.45 to 0.09 | 0.19 |
| $SPI_{pv}$ | 0.12 | −0.16 to 0.77 | 0.19 |
| $OSI_{pv}$ | – | – | – |
| Poiseuille, flow | | | |
| Mean $ESS_{pq}$ | −0.18 | −0.42 to −0.01 | 0.04 |
| $SPI_{pq}$ | 0.14 | −0.12 to 0.81 | 0.14 |
| $OSI_{pq}$ | 0.04 | −373.49 to 556.56 | 0.69 |

Linear regression analysis to assess the association between endothelial shear stress (ESS) values and mean wall thickness (MWT) adjusted for age and systolic blood pressure are shown (beta coefficients and 95 % confidence intervals of the unstandardized coefficients). SPI is shear pulsatility index, OSI is oscillatory shear index

**Table 3** Interscan measurement variability of endothelial shear stress estimations

| | ICC | 95 % CI | *P* |
|---|---|---|---|
| Velocity gradient modelling | | | |
| Mean $ESS_{vg}$ | 0.78 | 0.67–0.86 | <0.001 |
| $SPI_{vg}$ | 0.74 | 0.61–0.84 | <0.001 |
| $OSI_{vg}$ | 0.66 | 0.51–0.78 | <0.001 |
| Womersley, center line velocity | | | |
| Mean $ESS_{wv}$ | 0.86 | 0.78–0.92 | <0.001 |
| $SPI_{wv}$ | 0.62 | 0.47–0.76 | <0.001 |
| $OSI_{wv}$ | 0.75 | 0.62–0.84 | <0.001 |
| Womersley, flow | | | |
| Mean $ESS_{wq}$ | 0.84 | 0.75–0.90 | <0.001 |
| $SPI_{wq}$ | 0.80 | 0.70–0.88 | <0.001 |
| $OSI_{wq}$ | 0.73 | 0.60–0.83 | <0.001 |
| Poiseuille, center line velocity | | | |
| Mean $ESS_{pv}$ | 0.86 | 0.78–0.92 | <0.001 |
| $SPI_{pv}$ | 0.66 | 0.51–0.78 | <0.001 |
| $OSI_{pv}$ | – | – | – |
| Poiseuille, flow | | | |
| Mean $ESS_{pq}$ | 0.84 | 0.75–0.90 | <0.001 |
| $SPI_{pq}$ | 0.69 | 0.55–0.80 | <0.001 |
| $OSI_{pq}$ | −0.01 | −0.16 to 0.18 | N.S. |

Intraclass correlation coefficients (ICC, 95 % confidence interval) for all estimation methods are shown. ESS is endothelial shear stress, SPI is shear pulsatility index and OSI is oscillatory shear index

difference between the Womersley-based prediction and the velocity gradient method was limited to ~13 %. Such systematic deviation would not affect the relevance for clinical studies, as demonstrated by the significant correlation of mean ESS with MWT. Taken together, the data suggest that flow rate should be preferred over centerline velocity as input for estimation of mean ESS.

Temporal variations in ESS and notably a change in direction during part of the cycle have strong effects on endothelial biology towards a pro-atherogenic phenotype [1, 3, 28, 29]. The more than twofold difference in estimated SPI between Poiseuille and Womersley flow and the lack of correlation between Poiseuille-based SPI and OSI estimation and MWT demonstrate the necessity to account for blood inertia in pulsatility assessment. This is notably the case in peak systole, where a major deviation from a parabolic flow profile occurred. The supplementary material analysis shows the consistency of flow profiles under Womersley and Poiseuille.

Importantly, in Womersley flow, phases of negative ESS can co-exist with continuous forward flow and forward centerline velocity. In Poiseuille flow, this is not possible. Indeed, Womersley flow predicted a non-zero OSI in part of the cases, while for Poiseuille flow OSI was zero, in concordance with the absence of flow reversal in the studied non-stenotic common carotid arteries. The occurrence of a non-zero OSI in the Womersley predictions depends primarily on the balance of mean flow and the amplitude of the pulsatile components. Also, the SPI was defined as this balance. The correlations of the Womersley-predicted OSI and SPI with MWT strongly suggest that this balance is clinically relevant. Vascular stiffening and increased pulse pressure are conditions that would increase the pulsatile flow components and cause a non-zero OSI. A high mean flow would reduce the likelihood of a non-zero OSI. It remains to be established whether the correlation of low mean flow with thicker walls that we observed is in fact the consequence of reversal of ESS during the heart cycle.

A substantial difference remained between Womersley-based and gradient-based estimates of ESS pulsation. Extensive work on software phantoms has evaluated the accuracy and precision of a comparable velocity gradient technique as a function of scanning and resolution parameters [31], providing arguments for the accuracy of this method. However, in the absence of a golden truth in the current data, there is no straightforward way of

quantitating accuracy of any of the methods. We suspect that the bias is also in the gradient method. ESR is defined as the velocity gradient in an infinitesimal small space above the endothelial cells. This gradient quickly falls further away from the endothelium in notably dynamic flow. The gradient method, having a finite resolution, might thus underestimate ESS pulsatility and also miss local reversal of the direction. Womersley provides a continuous solution for velocity as function of distance from the endothelium, which under the assumption of no-slip should give an inherently better estimate of ESS pulsatility. The Womersley-based and gradient-based SPI correlated equally well with MWT, indicating that these differences do not affect the usefulness of either SPI estimate in clinical studies. However, the OSI, which relies on subtle changes of the flow in the boundary layer, only correlated with MWT for Womersley-based methods.

### Applicability

The current approach uses vascular diameter and either centerline velocity or flow rate as input, without requirement for more detailed data on the spatial velocity profile. Techniques that can provide such data include Echo-Doppler scanning and phase contrast MRI. The ability to estimate ESS from Echo-Doppler scanning allows implementation as pseudo-endpoint in large clinical studies. MRI methods based on direct measurement of local velocity vectors in 3D, such as 3D PC-MRI, may form a good approach for dedicated studies in complex geometries [32]. Yet, the current findings suggest that a much simpler implementation of Womersley-based estimation of shear parameters with consequently much shorter scanning times is a good alternative strategy in clinical studies on common carotid arteries.

All applied methods had good reproducibility. Reproducibility of the flow-based Womersley estimates for mean ESS and pulsatility exceeded that of the gradient modelling. While flow rate should be preferred over centerline velocity for mean ESS, for pulsatility (SPI and OSI) centerline velocity also provides a good correlation with MWT and good reproducibility, supporting the use of ultrasound or simple MRI protocols for pulsatility quantification.

### Limitations of the study

It is clear that the requirements for Womersley flow were violated to some degree. Recently, Mynard et al. [33] evaluated the consequences of carotid curvature on Poiseuille- and Womersley-based estimates for mean and peak ESS. In that study, computational fluid dynamics based on the Navier–Stokes equations were used as the gold standard. Their results indicate that even a slight curvature causes substantial bias and circumferential heterogeneity of these estimates. The effect of curvature on SPI or OSI was not tested. In the current study, we did not apply computational fluid dynamics, and it remains to be established to what extent deviations from a straight tube influence the pulsatile ESS parameters and their correlation with MWT. Computational fluid dynamics methods are, apart from being time-consuming, affected by errors in boundary conditions and geometry definitions, as well as by assumptions on wall rigidity and blood rheology, precluding their general use in large clinical studies.

In the absence of a gold standard for ESS in large clinical studies, evidence for usefulness of any ESS method comes from correlation with wall biology and thickening, and it seems reasonable to evaluate the accuracy of the ESS estimates from the correlation with MWT. The current correlation of Womersley-based mean ESS, SPI and OSI with MWT as a marker for atherosclerotic burden is not necessarily causal; longitudinal studies on predictive value of shear parameters for cardiovascular events should allow evaluating their usefulness as pseudo-endpoints in clinical studies.

## Conclusions

In the present study we developed a reproducible and accurate Womersley flow based method to estimate the endothelial shear stress dynamics in the common carotid arteries. We showed that this method is equally good as the more complex velocity gradient modelling method and superior to the simpler Poiseuille flow based method to estimate ESS. The Womersley based method we present solely requires the measurement of flow rate or centerline velocity and carotid artery diameter. This renders the method applicable for large clinical studies without the need for complex analyses and computations. While having its limitations, the Womersley based method should therefore replace the frequently used Poiseuille based method, enabling better assessment of the relationship between ESS, atherosclerosis and cardiovascular disease in future clinical studies.

**Acknowledgments** We would like to thank A.M. van den Berg for assisting in the data acquisition. JCVS was supported by Grant 01C-204 (EMINENCE project) from the Center for Translational Molecular Medicine.

**Conflict of interest** The authors declare that they have no conflict of interest.

## References

1. Davies PF (2009) Hemodynamic shear stress and the endothelium in cardiovascular pathophysiology. Nat Clin Pract Cardiovasc Med 6:16–26. doi:10.1038/ncpcardio1397

2. Tzima E, Irani-Tehrani M, Kiosses WB, Dejana E, Schultz DA, Engelhardt B, Cao G, DeLisser H, Schwartz MA (2005) A mechanosensory complex that mediates the endothelial cell response to fluid shear stress. Nature 437:426–431. doi:10.1038/nature03952
3. Dai G, Kaazempur-Mofrad MR, Natarajan S, Zhang Y, Vaughn S, Blackman BR, Kamm RD, García-Cardeña G, Gimbrone MA (2004) Distinct endothelial phenotypes evoked by arterial waveforms derived from atherosclerosis-susceptible and -resistant regions of human vasculature. Proc Natl Acad Sci USA 101:14871–14876. doi:10.1073/pnas.0406073101
4. Langille BL, O'Donnell F (1986) Reductions in arterial diameter produced by chronic decreases in blood flow are endothelium-dependent. Science 231:405–407. doi:10.1126/science.3941904
5. Duivenvoorden R, Vanbavel E, de Groot E, Stroes ES, Disselhorst JA, Hutten BA, Laméris JS, Kastelein JJ, Nederveen AJ (2010) Endothelial shear stress: a critical determinant of arterial remodeling and arterial stiffness in humans–a carotid 3.0-T MRI study. Circ Cardiovasc Imaging 3:578–585. doi:10.1161/CIRCIMAGING.109.916304
6. Gnasso A, Carallo C, Irace C, Spagnuolo V, De Novara G, Mattioli PL, Pujia A (1996) Association between intima-media thickness and wall shear stress in common carotid arteries in healthy male subjects. Circulation 94:3257–3262. doi:10.1161/01.CIR.94.12.3257
7. Irace C, Carallo C, De Franceschi MS, Scicchitano F, Milano M, Tripolino C, Scavelli F, Gnasso A (2012) Human common carotid wall shear stress as a function of age and gender: a 12-year follow-up study. Age 34:1553–1562. doi:10.1007/s11357-011-9318-1
8. Irace C, Cortese C, Fiaschi E, Carallo C, Farinaro E, Gnasso A (2004) Wall shear stress is associated with intima-media thickness and carotid atherosclerosis in subjects at low coronary heart disease risk. Stroke 35:464–468. doi:10.1161/01.STR.0000111597.34179.47
9. Katritsis D, Kaiktsis L, Chaniotis A, Pantos J, Efstathopoulos EP, Marmarelis V (2007) Wall shear stress: theoretical considerations and methods of measurement. Prog Cardiovasc Dis 49:307–329. doi:10.1016/j.pcad.2006.11.001
10. Oyre S, Ringgaard S, Kozerke S, Paaske WP, Erlandsen M, Boesiger P, Pedersen EM (1998) Accurate noninvasive quantitation of blood flow, cross-sectional lumen vessel area and wall shear stress by three-dimensional paraboloid modeling of magnetic resonance imaging velocity data. J Am Coll Cardiol 32:128–134. doi:10.1016/S0735-1097(98)00207-1
11. Ford MD, Xie YJ, Wasserman BA, Steinman DA (2008) Is flow in the common carotid artery fully developed? Physiol Meas 29:1335–1349. doi:10.1088/0967-3334/29/11/008
12. Box FM, van der Geest RJ, van der Grond J, van Osch MJ, Zwinderman AH, Palm-Meinders IH, Doornbos J, Blauw GJ, van Buchem MA, Reiber JH (2007) Reproducibility of wall shear stress assessment with the paraboloid method in the internal carotid artery with velocity encoded MRI in healthy young individuals. J Magn Reson Imaging 26:598–605. doi:10.1002/jmri.21086
13. Box FM, van der Grond J, de Craen AJ, Palm-Meinders IH, van der Geest RJ, Jukema JW, Reiber JH, van Buchem MA, Blauw GJ, Group PS (2007) Pravastatin decreases wall shear stress and blood velocity in the internal carotid artery without affecting flow volume: results from the PROSPER MRI study. Stroke 38(4):1374–1376. doi:10.1161/01.STR.0000260206.56774.aa
14. Womersley JR (1955) Method for the calculation of velocity, rate of flow and viscous drag in arteries when the pressure gradient is known. J Physiol 127:553–563
15. Friedman MH, Hutchins GM, Bargeron CB, Deters OJ, Mark FF (1981) Correlation between intimal thickness and fluid shear in human arteries. Atherosclerosis 39:425–436. doi:10.1016/0021-9150(81)90027-7
16. Li C, Kao C-Y, Gore JC, Ding Z (2007) Implicit active contours driven by local binary fitting energy. In 06(2007):1–7. doi:10.1109/CVPR.2007.383014
17. Reneman RS, Arts T, Hoeks AP (2006) Wall shear stress–an important determinant of endothelial cell function and structure–in the arterial system in vivo. Discrepancies with theory. J Vasc Res 43:251–269. doi:10.1159/000091648
18. Ku DN, Giddens DP, Zarins CK, Glagov S (1985) Pulsatile flow and atherosclerosis in the human carotid bifurcation. Positive correlation between plaque location and low oscillating shear stress. Arterioscler Thromb Vasc Biol 5:293–302. doi:10.1161/01.ATV.5.3.293
19. Adame IM, van der Geest RJ, Bluemke DA, Lima JA, Reiber JH, Lelieveldt BP (2006) Automatic vessel wall contour detection and quantification of wall thickness in in vivo MR images of the human aorta. J Magn Reson Imaging 24:595–602. doi:10.1002/jmri.20662
20. Duivenvoorden R, de Groot E, Elsen BM, Laméris JS, van der Geest RJ, Stroes ES, Kastelein JJ, Nederveen AJ (2009) In vivo quantification of carotid artery wall dimensions: 3.0-Tesla MRI versus B-mode ultrasound imaging. Circ Cardiovasc Imaging 2:235–242. doi:10.1161/CIRCIMAGING.108.788059
21. Ugron Á, Paál G (2014) On the boundary conditions of cerebral aneurysm simulations. Periodica Polytechnica Mech Eng 58(1):37–45. doi:10.3311/PPme.7392
22. Taylor CA, Steinman DA (2010) Image-based modeling of blood flow and vessel wall dynamics: applications, methods and future directions: sixth international bio-fluid mechanics symposium and workshop, March 28–30, 2008 Pasadena, California. Ann Biomed Eng 38:1188–1203. doi:10.1007/s10439-010-9901-0
23. Remuzzi A, Ene-Iordache B, Mosconi L, Bruno S, Anghileri A, Antiga L, Remuzzi G (2003) Radial artery wall shear stress evaluation in patients with arteriovenous fistula for hemodialysis access. Biorheology 40:423–430
24. Simon AC, Levenson J, Flaud P (1990) Pulsatile flow and oscillating wall shear stress in the brachial artery of normotensive and hypertensive subjects. Cardiovasc Res 24:129–136. doi:10.1093/cvr/24.2.129
25. Stroev PV, Hoskins PR, Easson WJ (2007) Distribution of wall shear rate throughout the arterial tree: a case study. Atherosclerosis 191:276–280. doi:10.1016/j.atherosclerosis.2006.05.029
26. Struijk PC, Stewart PA, Fernando KL, Mathews VJ, Loupas T, Steegers EAP, Wladimiroff JW (2005) Wall shear stress and related hemodynamic parameters in the fetal descending aorta derived from color Doppler velocity profiles. Ultrasound Med Biol 31:1441–1450. doi:10.1016/j.ultrasmedbio.2005.07.006
27. Holdsworth DW, Norley CJ, Frayne R, Steinman DA, Rutt BK (1999) Characterization of common carotid artery blood-flow waveforms in normal human subjects. Physiol Meas 20:219–240. doi:10.1088/0967-3334/20/3/301
28. Brooks AR, Lelkes PI, Rubanyi GM (2002) Gene expression profiling of human aortic endothelial cells exposed to disturbed flow and steady laminar flow. Physiol Genomics 9:27–41. doi:10.1152/physiolgenomics.00075.2001
29. Malek AM, Alper SL, Izumo S (1999) Hemodynamic shear stress and its role in atherosclerosis. JAMA 282:2035–2042. doi:10.1001/jama.282.21.2035
30. Chatzizisis YS, Coskun AU, Jonas M, Edelman ER, Feldman CL, Stone PH (2007) Role of endothelial shear stress in the natural history of coronary atherosclerosis and vascular remodeling: molecular, cellular, and vascular behavior. J Am Coll Cardiol 49:2379–2393. doi:10.1016/j.jacc.2007.02.059
31. Potters WV, van Ooij P, Marquering H, Vanbavel E, Nederveen AJ (2014) Volumetric arterial wall shear stress calculation based

on cine phase contrast MRI. J Magn Reson Imaging 1–12. doi:10.1002/jmri.24560
32. van Ooij P, Potters WV, Guédon A, Schneiders JJ, Marquering HA, Majoie CB, vanBavel E, Nederveen AJ (2013) Wall shear stress estimated with phase contrast MRI in an in vitro and in vivo intracranial aneurysm: WSS in Intracranial Aneurysms. J Magn Reson Imaging 38:876–884. doi:10.1002/jmri.24051
33. Mynard JP, Wasserman BA, Steinman DA (2013) Errors in the estimation of wall shear stress by maximum Doppler velocity. Atherosclerosis 227:259–266. doi:10.1016/j.atherosclerosis.2013.01.026